

TIFR/TH/97-03

January, 1997

hep-ph/yymmdd

Thermal Effects on Two-photon Decays of Pseudo-scalars

Sourendu Gupta¹ and S. N. Nayak²Theory Group, Tata Institute of Fundamental Research,
Homi Bhabha Road, Bombay 400005, India.

Abstract

We study the effect of finite temperatures and Fermion density on the effective pseudo-scalar-photon vertex induced by the triangle diagram. The manifestly covariant calculations show that when the pseudo-scalar mass is much less than the temperature, then there is a large enhancement of the decay rate. Alternatively, when the temperature is much higher than the Fermion mass, or the Fermion chemical potential is large, the lifetime is enhanced. Other related processes, and applications of these results to cosmology and astrophysics, are discussed.

¹E-mail: sgupta@theory.tifr.res.in

²E-mail: nayak@theory.tifr.res.in

1 Introduction

Goldstone Bosons arise in field theories when some global symmetry is spontaneously broken. A solution of the strong CP problem involves the breaking of Peccei-Quinn symmetry and gives rise to a pseudo-scalar called the axion (A) [1], which becomes massive through mixing with the pion. Axions have couplings to charged Fermions and are candidate dark matter which could play an important role in cosmology [2]. The physics of axions involves two intrinsic mass scales— the axion mass, M , and the Fermion mass, m . If axions participate in physics inside a heat bath with temperature, T , larger than any one of (or both) these scales, then we may expect interesting and non-trivial thermal effects. Since the mass of the axion can be much less than the cosmic microwave background temperature ($T_b = 2.7$ K), even the coldest environment in the universe may be thermal in this sense. The purpose of this paper is to identify the main sources of non-trivial thermal effects.

We compute the decay rate of the axion into two photons through the triangle diagram and find two sources of thermal effects. Stimulated emission of final state photons enhances the decay width of the pseudo-scalar, and plays the dominant role in the physics of axions for $M < T_b$. Pauli blocking of on-shell parts of the Fermions in the loop reduces the decay width when $T > m$, and may have interesting consequences in the physics of supernovæ. These changes in the effective $A\gamma\gamma$ vertices also contribute to the Primakoff effect, $\gamma e \rightarrow Ae$ through a t -channel photon exchange. Thermal effects can also boost the multi-photon channels to a very large extent and may require a resummation of this whole class of processes.

One bit of physics is worth emphasizing. At $T = 0$ the decay width, Γ , depends on all the scalars in the problem. These are the masses M and m . The momenta of the decay photons, k_1 and k_2 ($k_1 + k_2 = q$, the momentum of A) do not contribute anything else, since $k_1 \cdot k_2 = M^2$. There are major changes in the kinematics at finite temperature, since the heat bath selects out a preferred frame. A covariant description can be retained in finite temperature field theory, provided an extra vector is introduced into the problem— the velocity of the heat-bath with respect to the frame in which one chooses to work, u ($u^2 = 1$) [3]. The amplitude may now depend on all the scalars in the problem. There are four new scalars— the temperature T , the Fermion chemical potential μ , and two scalar-products, which can be chosen as $q \cdot u$ and $k_1 \cdot u$. Since Γ is obtained after integration over the

two-photon phase space, the dependence on $k_1 \cdot u$ drops out. Consequently, Γ is a function of M , m , T , μ and $q \cdot u$. This last quantity is the energy of A in the rest frame of the heat-bath.

A simple representation of the new invariants facilitates the discussions in the later sections. Evaluate them in the rest frame of A , $q = (M, 0, 0, 0)$. Align u along the z -direction and write $u = (\gamma, 0, 0, \beta)$. Since the energy of each photon is $M/2$, and the momenta balance,

$$\begin{aligned} q \cdot u &= M\gamma, \\ k_1 \cdot u &= \frac{1}{2}M\gamma(1 - \beta \cos \chi), \\ k_2 \cdot u &= \frac{1}{2}M\gamma(1 + \beta \cos \chi). \end{aligned} \tag{1.1}$$

It is now obvious that γ and χ are Lorentz invariants. Also, $\beta = \sqrt{(1 - 1/\gamma^2)}$ can be interpreted as the boost between the rest frames of A and the heat-bath.

The plan of this paper is the following. In Section 2 we present the calculation of the triangle diagram at $T > 0$, compute the decay width, and discuss some applications of these results. The next section contains a discussion of other related processes, including the Bose enhancement of multi-photon decays. Some field-theoretic points are discussed in the appendix.

2 The Triangle Diagram at $T > 0$.

In this section we compute the triangle diagram at $T > 0$. A limiting case, $\gamma = 1$, has been considered before [5]. In all physical applications it is appropriate to consider the limit $M \ll m$. The photon-Fermion coupling is taken to be $ie\hat{\varepsilon}(k)$ (for any vector p we denote $\hat{p} = \gamma_\mu p^\mu$), where $\varepsilon(k)$ denotes the polarisation vector of a photon of momentum k . The Fermion- A coupling is $ig\gamma_5$.

We summarise the computation of the decay width at $T = 0$. The matrix element, \mathcal{M} , coming from the triangle diagram, has the form

$$\mathcal{M} = -\frac{ge^2}{4\pi^4} \varepsilon^\mu(k_1) \varepsilon^\nu(k_2) T_{\mu\nu} f(M, m) \quad \text{where} \quad T_{\mu\nu} = m \varepsilon_{\mu\nu\sigma\rho} k_1^\sigma k_2^\rho. \tag{2.1}$$

The Lorentz-scalar, f , is a form-factor for the effective $A\gamma\gamma$ vertex and is obtained as an integral over the Fermion-loop momentum. It is a function

only of M and m . It is possible to expand f as

$$f(M, m) = f_0(m) + z^2 f_1(m) + \dots, \quad (z = \frac{M}{2m}). \quad (2.2)$$

A text-book calculation gives $f_0 = -\pi^2/m^2$ and $f_1 = -\pi^2/3m^2$ [6]. The decay width, Γ , is computed by integrating the squared matrix element over the Lorentz-invariant phase space of the final state—

$$\Gamma(M, m) = \left(\frac{\alpha^2 g^2}{16\pi^3} \right) z^2 M. \quad (2.3)$$

In the usual formulation of finite-temperature field theory [7], the physical fields (called type 1) are doubled by the addition of so-called “thermal ghosts” (type 2 fields). Each vertex involves only one type of fields. External legs connect only to type 1 vertices. Each propagator may connect any two types of vertices and hence becomes a 2×2 matrix which can easily be written down in terms of advanced and retarded Green’s functions along with the Bose or Fermi distributions. In the triangle diagram all vertices connect to external legs, and we need to consider only the type 11 Fermion propagators [8]

$$\mathcal{D}(p, u) = (\hat{p} + m) \left[\frac{1}{p^2 - m^2 + i\epsilon} + 2\pi i \delta(p^2 - m^2) \times \right. \\ \left. \{ \Theta(p_0) F^+(p \cdot u) + \Theta(-p_0) F^-(p \cdot u) \} \right], \quad (2.4)$$

where a regulator has been placed in the denominator of the propagator, $F^\pm(x) = 1/(\exp(|x| \mp \mu)/T + 1)$, and μ is the Fermion chemical potential. Note that this is the sum of a $T = 0$ and a $T > 0$ part. It is convenient to use a diagrammatic notation where the $T = 0$ part is denoted by a line and the $T > 0$ part by a line with a cut. Thermal effects on external legs can be subsumed into Bose and Fermi distributions multiplying the phase space volume element. We return to this point in the appendix.

2.1 The Form Factor

Note that the Dirac structure of the propagator is the same as at $T = 0$. As a result, the tensor structure of the matrix element remains as in eq. (2.1)

and the only thermal effects come from the form factor f and the photon phase space. The modified form factor is

$$f = \int d^4p \mathcal{D}(p) \mathcal{D}(p - k_1) \mathcal{D}(p - q). \quad (2.5)$$

Separating the $T = 0$ and $T > 0$ parts of the propagator, the thermal form factor has eight terms. Apart from the $T = 0$ contribution, other terms can be grouped as (a) one term with the thermal part of all three propagators (b) three terms with the thermal part of any two and (c) three terms with the thermal part of only one propagator. For $M < 2m$ and $m > 0$, the three mass-shell conditions in (a) leave no phase-space volume to the integral and hence this contribution is identically zero. For the same reason each term in (b) is also zero. Consequently, the thermal contribution comes only from (c), written in a diagrammatic notation as

$$f = 2 \left(q \left\langle \begin{array}{c} \mu, k_1 \\ p \\ \nu, k_2 \end{array} \right\rangle + q \left\langle \begin{array}{c} \mu, k_1 \\ p \\ \nu, k_2 \end{array} \right\rangle + q \left\langle \begin{array}{c} \mu, k_1 \\ p \\ \nu, k_2 \end{array} \right\rangle \right) \quad (2.6)$$

$$= 2(J_1 + J_2 + J_3).$$

The factor of two comes from the diagrams obtained by simultaneous interchange of μ, ν and k_1, k_2 .

Each of the integrals J_i can be reduced to a Lorentz invariant one-dimensional Fermi integral. We show some of the details for J_1 , to demonstrate that the computation can be performed covariantly. After shifting $p \rightarrow p + k_1$, and introducing a resolution of identity as a sum over positive and negative energy Θ -function, J_1 reduces to a simple integral over a real particle phase space

$$J_1 = -\pi \int \frac{d^3p}{2p_0} (F^-(x) + F^+(x)) \frac{1}{p \cdot k_1 p \cdot k_2} \quad (2.7)$$

This integral is finite and well-defined for $m > 0$, and, being a Lorentz-scalar, may be evaluated in any convenient frame. We use the frame where $u = (1, 0, 0, 0)$. In this frame $p_0 = p \cdot u$ is a Lorentz-scalar. As a result,

$\mathbf{p}^2 = p_0^2 - m^2$ is also invariant, and all the manipulations shown here are explicitly Lorentz invariant.

First we use the Feynman trick to write

$$J_1 = -\frac{\pi}{2} \int \frac{d\mathbf{p} \mathbf{p}^2}{p_0} [F^-(p_0) + F^+(p_0)] \Omega_1, \quad \text{where} \quad \Omega_1 = \int \frac{d\alpha d\Omega}{(p \cdot V)^2} \quad (2.8)$$

Here α is the Feynman parameter ($0 \leq \alpha \leq 1$) and $V = \alpha k_1 + (1 - \alpha)k_2$. We choose the orientation of the frame by setting $V = (V_0, 0, 0, V_3)$. Since $V_0 = V \cdot u$, both V_0 and V_3 are Lorentz-invariant. The angular integral is easily performed, leaving $\Omega_1 = (4\pi/M^2) \int d\alpha/Q_1(\alpha)$, where the $Q_1(\alpha)$ is a quadratic in α with Lorentz-invariant coefficients. It is easy to check that the two roots of Q_1 do not lie in the range of integration. Then the integral over α is easily performed. With the notation

$$\mathcal{P}^2 = \mathbf{p}^2 + m^2 \gamma^2 (1 - \beta^2 \cos^2 \chi), \quad (2.9)$$

we have the compact expression

$$J_1 = -\frac{4\pi^2}{M^2} \int_0^\infty \frac{d\mathbf{p} \mathbf{p}}{p_0 \mathcal{P}} [F^-(p_0) + F^+(p_0)] \log \left(\frac{\mathcal{P} + \mathbf{p}}{\mathcal{P} - \mathbf{p}} \right). \quad (2.10)$$

J_2 and J_3 can be obtained in a similiar fashion.

The $T > 0$ result may be exhibited in a form similiar to that in eq. (2.2) by expanding the integrals in a series in $z = M/2m$. Each of the integrals J_i ($i = 1, 2, 3$) has an overall factor of $1/M^2$. The only M dependence of J_1 is in this factor. The expansion of $J_2 + J_3$, starts at order $1/z$. A straightforward check shows that the first term of the expansion precisely cancels J_1 . The first non-zero term is of order z^0 and this is followed by a series in z^2 . All these terms in the expansion come entirely from $J_2 + J_3$.

We give here the final result for the full T -dependent f_0 —

$$\begin{aligned} f_0(M, m, \mu, T, \gamma) = & -\frac{\pi^2}{m^2} + \frac{\pi^2 \gamma^2}{m^2} \int_0^\infty \frac{dr r}{r_0 R^5} [F^-(\zeta r_0) + F^+(\zeta r_0)] \\ & \times \left[(2r_0^2 - \gamma^2 \beta^2 \sin^2 \chi) \left\{ (1 + \bar{\beta}^2) \log \left(\frac{R+r}{R-r} \right) \right. \right. \\ & \left. \left. - 2\bar{\beta} \log \left(\frac{R+r\bar{\beta}}{R-r\bar{\beta}} \right) \right\} \right. \\ & \left. - \frac{2rR}{r^2 + \gamma^2} (2r_0^2 \bar{\beta}^2 - (r^2 + \gamma^2) \beta^2 \sin^2 \chi) \right], \quad (2.11) \end{aligned}$$

where $\bar{\beta} = \beta \cos \chi$, $r_0^2 = 1 + r^2$, $R^2 = r^2 + \gamma^2(1 - \bar{\beta}^2)$, and $\zeta = m/T$. This complicated looking result may be simplified in various limits, or evaluated numerically (see Figure 1).

An instructive limit is $\gamma \rightarrow 1$, *i. e.*, the special case when A is at rest in the rest-frame of the heat bath, and $\mu = 0$ —

$$f(M, m, T) = -\frac{\pi^2}{m^2} + \frac{2\pi^2}{m^2} \int_0^\infty \frac{r dr}{r_0^4} \log\left(\frac{r_0 + r}{r_0 - r}\right) \frac{1}{e^{\zeta r_0} + 1}. \quad (2.12)$$

This result agrees with previous expressions obtained in this limit [5].

It is also interesting to see that in the limit $T \gg m$, the integral takes on the value 1/2 and the thermal part of f precisely cancels the $T = 0$ result, giving $f = 0$. Thus the decay width vanishes in the joint limits $\beta \rightarrow 0$ and $M \ll m \ll T$. The reason is quite simple. A close perusal of the $T = 0$ calculation shows that f picks up a non-vanishing contribution only from that part of the phase space where one of the Fermions is on-shell. This contribution is fully Pauli-blocked in the limit $T \gg m$.

For $m \ll T$ it is useful to perform an expansion of the form factor f . From eq. (2.12) it is clear that

$$f = -\frac{\pi^2 \zeta}{2m^2} \int_0^\infty \frac{r dr}{r_0^3} \log\left(\frac{r_0 + r}{r_0 - r}\right) + \mathcal{O}(\zeta^2) \sim -0.7707\zeta \left(\frac{\pi^2}{m^2}\right) \quad (2.13)$$

In the other limit, $m \gg T$, the thermal contribution vanishes exponentially in ζ , leaving f to take on its $T = 0$ value.

The results are even simpler when A travels very fast through the medium, *i.e.*, in the limit $\gamma \rightarrow \infty$. In this limit the quadratics appearing in the definitions of all the J 's go as γ^2 . Hence the thermal contribution vanishes as $1/\gamma^2$, and the matrix element is equal to its $T = 0$ limit.

2.2 The decay width

Next we construct the decay width for $A \rightarrow \gamma\gamma$. In addition to the matrix element computed in the previous section, we require the 2-body decay phase space for $T > 0$. This contains a factor $1 + B(k \cdot u)$ for each photon (due to stimulated emission in the heat-bath), where $B(x) = 1/(\exp |x| - 1)$ is the Bose distribution function. Then, after the usual reduction of the 2-body

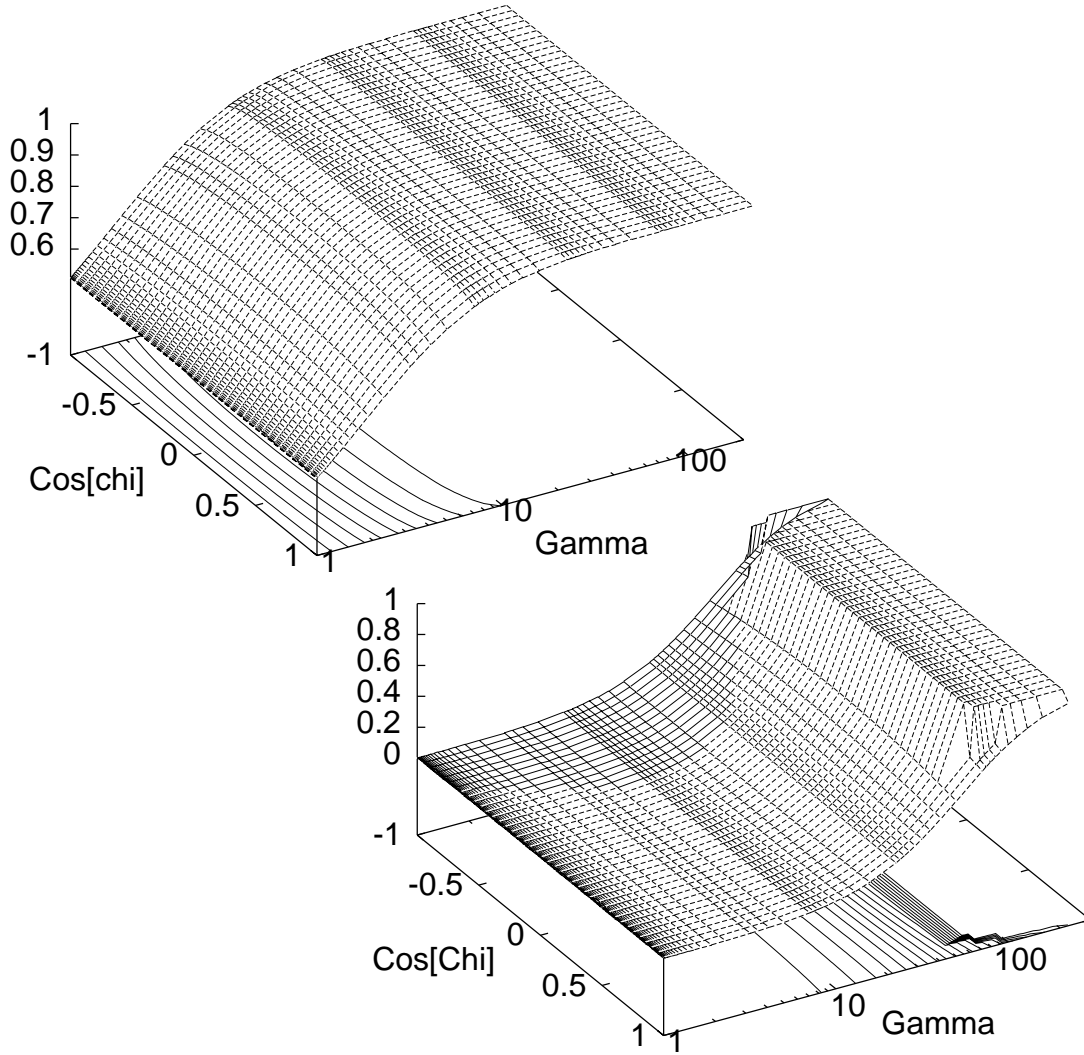


Figure 1: The form-factor $|f_0 m^2 / \pi^2|$ shown as a function of γ and $\cos \chi$ for values of T and μ appropriate to a supernova core ($T = 40$ MeV, $\mu = 450$ MeV; lower panel) and the neutrino-sphere in a supernova ($T = 1$ MeV, $\mu = 0$; upper panel). Isolines drawn on the γ - $\cos \chi$ plane correspond to function values increasing in steps of 0.05 upto a largest value (on the right) of 0.95.

phase space,

$$\Gamma(M, m, \mu, T, \gamma) = \frac{g^2 \alpha^2 m^2 M^3}{128 \pi^7} \int_{-1}^1 d \cos \chi f^2(M, m, \mu, T, \gamma, \chi) [1 + B(k_1 \cdot u)] [1 + B(k_2 \cdot u)]. \quad (2.14)$$

For the value of f calculated in the previous section, the integral has to be performed numerically for general values of the argument.

When the χ -dependence of the form factor can be neglected, the thermal effect arises entirely from the phase space factors. In this case the decay width is

$$\Gamma(M, m, \mu, T, \gamma) = \frac{g^2 \alpha^2 m^2 M^3 f^2}{64 \beta \xi \pi^7} \left(\frac{1}{1 - e^{-2\xi}} \right) \left[\beta \xi - \log \left(\frac{e^{(1+\beta)\xi} - 1}{e^{(1-\beta)\xi} - 1} \right) \right], \quad (2.15)$$

where $\xi = M\gamma/2T$. For $\beta \rightarrow 0$ and $M \ll T$, we find that Γ is the $T = 0$ width times T^2/M^2 . On the other hand, for $T \ll M$ we recover the $T = 0$ result. For general values of the parameters a numerical integration of the expression in eq. (2.14) is required.

The physics of the temperature dependence of the decay width can be summarised as—

1. For $T \ll M \ll m$ or large β , thermal effects can be neglected and the decay width is the same as at $T = 0$.
2. For small β and $M \ll T \ll m$ the dominant effect is the stimulated emission of final state photons, leading to a highly enhanced decay rate.
3. For small β $M \ll m \ll T$ Pauli blocking of the on-shell part of the loop determines the physics and the decay rate is reduced.

2.3 Some Applications

The simple computations above can be used to bound M . A large effect comes from the fact that $\Gamma \sim M^3$ at $T = 0$, whereas $\Gamma \sim T^2 M$ for $M \leq T$. This thermal enhancement of the decay width has an interesting consequence when $M \ll T_b = 0.235 \times 10^{-3}$ eV. The $T = 0$ result, in conjunction with some cosmological arguments, would predict a bound on $g < c/M^{3/2}$, whereas

the $T > 0$ results strengthen this to $g < c'/\sqrt{M}$ (c and c' are computable constants).

If A is to be a candidate for cold dark matter, then $\beta \approx 0$ and the lifetime must be greater than the age of the universe, t_0 [2]. Then

$$g \leq \left(\frac{8\pi\bar{m}}{\alpha M} \right) (1 - e^{-M/2T_b}) \sqrt{\frac{\pi}{Mt_0}} \quad (2.16)$$

where the average Fermion mass $\bar{m}^{-2} = \sum_f m_f^{-2}$ is dominated by the lightest flavour, the electron. Assuming the present age of the universe to be 15×10^9 years, we find that when $M \gg T_b$, $c = 1.2 \times 10^{-7} \text{ eV}^{3/2}$ and when $M \ll T_b$, $c' = 2.5 \times 10^{-4} \text{ eV}^{1/2}$.

The coupling g also can be constrained by the condition that the energy density of the decay photons is limited by observation of the micro-wave background, ρ_γ . We will assume [9] that A is produced non-thermally in the early universe. Then we can use the decay width in the limit $\beta \rightarrow 0$. The additional photon energy density due to the decay of A at present is

$$\Delta\rho_\gamma(t) = \bar{\rho}_A(t) [1 - e^{-\Gamma(t-t_i)}], \quad (2.17)$$

where t_i is the production epoch and $\bar{\rho}_A$ is the energy density which would have remained with A in the absence of decays. Now $\Delta\rho_\gamma \leq \rho_\gamma$, and $\bar{\rho}_A$ must be greater than the present critical density ρ_{cr} [9]. Since $t_i \ll t$, we find

$$g \leq \left(\frac{8\pi\bar{m}}{\alpha M} \right) (1 - e^{-M/2T_b}) \sqrt{\frac{-\pi \log(1 - \rho_\gamma/z\rho_{cr})}{Mt_0}} \quad (2.18)$$

Taking $\rho_A = z\rho_{cr}$ with $z = 0.9$, $\rho_\gamma = 0.260 \text{ eV/cm}^3$, $\rho_{cr} = 1.054 \times 10^{-5} h_0^2 \text{ GeV/cm}^3$ and choosing $h_0 = 0.85$ (to get the weakest bound), we find that $c = 7.1 \times 10^{-10} \text{ eV}^{3/2}$ and $c' = 1.5 \times 10^{-6} \text{ eV}^{1/2}$.

On the other hand, if we assume that $\Delta\rho_\gamma$ at the present epoch is smaller than the known error induced through the error on the COBE measurement of T_b , then the constraints are harder by a factor of 0.04. This gives $c = 2.8 \times 10^{-11} \text{ eV}^{3/2}$ and $c' = 6 \times 10^{-8} \text{ eV}^{1/2}$. In all these cases the bound on g is sharpened by two orders of magnitude through the leading order diagram alone. Although this does not place very stringent restrictions on axion models, in the next section we consider higher order diagrams and argue that they may lead to even sharper bounds.

Apart from axion models, these computations can also be used to bound the couplings and masses of any other pseudo-scalar with a γ_5 vertex to charged Fermions. One such model, which is not ruled out by data, is a singlet-triplet Majoron model [10]. This Majoron is a Goldstone Boson for Lepton number breaking and may be given a mass through couplings to gravity [11]. Since this mechanism typically produces low masses, the thermal bound is applicable.

Another class of limits arises from consideration of the cooling rates of stars from emission of pseudo-scalars. Our computation of the form factor is applicable to this situation, not only through the direct two-photon channel, but also through the Primakoff process. Thermal effects in most stars are rather small, due to the fact that $T \ll m$. However, they can be important in supernovæ since the $A\gamma\gamma$ vertex is suppressed (see Figure 1). This may affect bounds on axions from supernova cooling rates[12, 13].

3 Other Processes.

3.1 Multi-photon decays

We have computed thermal effects on the decay width of a pseudo-scalar (of mass M) in the two-photon channel through the triangle diagram with charged Fermions of mass m circulating in the loop. We found a strong increase in the decay width due to Bose enhancement of the final state photons for $M < T \ll m$, leading to a sharpening of the bound on the coupling between the pseudo-scalar and Fermions by two orders of magnitude for $M = 10^{-5}$ eV. Multi-photon decays are likely to yield more stringent bounds.

The total width of the axion into multi-photon channels at $T = 0$ can be written as the perturbation series

$$\Gamma = \alpha^2\Gamma_2 + \alpha^4\Gamma_4 + \dots \quad (3.1)$$

Since $\alpha^2 \approx 10^{-4}$, the series converges extremely fast and even the second term can be neglected. However, the situation changes at finite temperature. The higher order terms, involving multi-photon decays are enhanced due to Bose factors on each external photon leg, and some of these may compensate the damping due to the fine structure constant.

Examine the case of a pseudo-scalar decaying into $2n$ photons, where the i -th photon momentum is k_i . When each $k_i \sim M/2n$, the Bose factors go as $(2nT/M)^{2n}$. As a result, the contribution of this process to the total decay width is

$$\alpha^{2n}\Gamma_{2n} = g^2\alpha^{2n}\frac{c_n}{(2n)!}\left(\frac{2nT}{M}\right)^{2n}M\left(\frac{M}{m}\right)^{2n}. \quad (3.2)$$

The last factor comes from propagators and the Dirac trace, the factorial is due to photon counting and c_n is essentially the dimensionless contribution due to the Fermion loop integral. Clearly, this region of phase space is not very important at higher orders since $T \ll m$.

However, in the part of phase space where one or more $k_i \rightarrow 0$ the Bose factors can become arbitrarily large. This can happen for $n \geq 2$. It is easy to check that the real $2n$ photon emission diagrams give non-vanishing amplitudes in this region of phase space. This is not the usual Bloch-Nordsieck problem, since the $T = 0$ width is perfectly well defined and insensitive to the infra-red (as long as $m > 0$). We expect these putative divergences to cancel when thermal ghosts and virtual corrections are taken into account. The result is that, the decay width at $T > 0$ is infra-red sensitive and hence must be resummed over all numbers of photons. Demonstrating the cancellation and extracting the finite parts, prior to summing the series then requires the full power of thermal field theory. This work is under progress and will be reported elsewhere.

3.2 Stellar Cooling

Stellar cooling arguments are dependent on the coupling of axions to matter. For small couplings axions stream out of the star, carrying energy. At larger couplings, the mean-free path may be smaller than the radius of the star, and an axio-sphere may form. Axions escape only from the surface of the axio-sphere.

We have seen that the axion-photon form factor decreases significantly at temperatures appropriate to the core of supernovæ. This does not have a significant effect on the cooling rate due to low-mass axions, since the decrease affects only the low-energy end of the spectrum. For small M the energy loss due to low-energy axions is negligible and large changes in production rate can be tolerated.

The main effect is seen for M large enough that an axio-sphere may be formed. Apart from the decrease in the form factor, one should also take into account changes in the pion decay constant, f_π , and the pion mass, m_π , since they enter the axion coupling. At $T \approx 40$ MeV, chiral perturbation theory shows some decrease in both these quantities [14]. Further, suppression of interaction rates of low-energy axions with leptons or hadrons, due to Pauli blocking, increases the mean-free path of low-energy axions. The net effect is that low-energy axions may escape from the core. At the same time, high-energy axions are converted to low energies by processes such as $Ae \rightarrow Ae$ (Compton). The inverse process of boosting the energy of the axions is suppressed by Pauli blocking and the falling density of low-energy axions. This may lead to a destabilisation of the axio-sphere. Quantitative estimates of the relaxation time for this instability and the equilibrium phase space distribution of axions will be detailed elsewhere.

Even in parts of parameter space where this instability is negligible, estimates of the axio-sphere radius and the critical coupling at which it forms necessitate a full thermal field theory computation. The radius of the axio-sphere is closely related to the relaxation time (and the mean free path length) of the axion. The relaxation rate is the difference of the production and decay rates (see the appendix) and is given by the imaginary part of the axion two-point function. This quantity is strongly affected by hard thermal loops, if the mass of the axion is less than $\sqrt{\alpha}T$. Assuming $T \approx 40$ MeV, treatments of axions with mass less than about 4 MeV in the supernova core require hard thermal loop resummation.

A Some Field-theoretic Niceties.

In Section 2 we have written down rules for computation of $T > 0$ decay widths which look very similar to those at $T = 0$. The formalism for doing this is developed in [15, 16]. We summarise the results in this appendix and show that our techniques are justified.

In general one computes decay rates by writing down cutting rules for loop contributions to a two-point function. At $T > 0$ loop diagrams require

the matrix propagator [7]

$$\begin{aligned}
iG(p) &= U(T, p) \begin{pmatrix} S(p) & 0 \\ 0 & S^*(p) \end{pmatrix} U(T, p), \\
S(p) &= \frac{i}{p^2 - m^2 + i\epsilon}, \\
U(T, p) &= B(p \cdot u) \begin{pmatrix} 1 & \frac{1}{2} \exp |p \cdot u| \\ \frac{1}{2} \exp |p \cdot u| & 1 \end{pmatrix}, \\
iG^\pm(p) &= 2\pi\delta(p^2 - m^2) [\Theta(\pm p_0) + B(p \cdot u)].
\end{aligned} \tag{A.1}$$

These rules for Bosons can be generalised in a similar form to Fermions and Gauge Bosons. At $T = 0$ the matrix is diagonal and only the $\Theta(\pm p_0)$ term appears on G^\pm .

The $T = 0$ notion of cutting a line is generalised at $T > 0$ to the notion of ‘‘circling’’ a vertex [15]. If a G_{11} line is circled only at one end, then it is replaced by G^+ if the momentum flows to the circled vertex (G^- otherwise). For a G_{22} line the rule is reversed, and the off-diagonal lines are left untouched. Since the off-diagonal terms are absent at $T = 0$, only Θ -functions appear on such lines, and these reproduce the familiar cuts.

Furthermore [16], the imaginary part of the self-energy can be written as

$$\text{Im } \Pi(p) = p \cdot u \Gamma_r(p \cdot u) = p \cdot u (\Gamma - \Gamma_p), \tag{A.2}$$

where Γ_r is the relaxation rate, Γ_p is the production rate of the particle in the heat bath and Γ is the computed decay rate.

Now, for the decay rate, we require that the particles in the loop are observed in the final state. We might guess that the computation requires the replacement

$$iG^\pm(p) = 2\pi\delta(p^2 - m^2)\Theta(\pm p_0) [1 + B(p \cdot u)]. \tag{A.3}$$

The overall factor of Θ allows us to talk of cut lines as at $T = 0$. Similarly, for the production rate we might guess that the replacement,

$$iG^\pm(p) = 2\pi\delta(p^2 - m^2)\Theta(\mp p_0) [1 + B(p \cdot u)], \tag{A.4}$$

is called for. Then do we miss cross terms which involve a $\theta(p_0)\theta(-p'_0)$? A simple check reveals that if the two-point function involves a real on-shell particle, then such cross terms vanish due to kinematical reasons. This is the

content of eq. (A.2), and the justification for the prescription in eq. (A.3), used in Section 2.

In our computation of the decay width, Γ , we have neglected hard thermal loops [4], corresponding to screening of electric charges. Knowing that they are important for computations of the photon self-energy at $T > 0$, for $k \cdot u \sim eT$, is their neglect justified? The answer is: yes, because these have large contributions to Γ_r , but their effect on Γ_p and Γ separately are small. We give the outline of a demonstration below.

The hard thermal loop contributions to the process we are interested in can be represented as

The diagram shows a triangle loop structure. Two vertices are represented by grey ovals labeled 'a' and 'b'. The top edge of the triangle is a wavy line labeled with momentum k_1 , with indices μ and σ at its ends. The bottom edge is a wavy line labeled with momentum k_2 , with indices ν and ρ at its ends. The left side of the triangle is a dashed line connecting vertex 'a' to vertex 'b'. The right side is also a dashed line connecting vertex 'b' to vertex 'a'. The equation is labeled (A.5).

The blobs represent all vertex corrections to the triangle diagram and self energy corrections to the Fermion and photon lines. The result is, retaining only the terms of interest,

$$\begin{aligned}
\Gamma^{(ab)} &= \int d^4k_1 d^4k_2 M_{\mu\nu}^{(a)} M_{\sigma\rho}^{(b)} \text{Im}\Pi_{\mu\sigma}(k_1) \text{Im}\Pi_{\nu\rho}(k_2) \\
&\sim \int d^4k_1 d^4k_2 [1 + B(k_1 \cdot u)] [1 + B(k_2 \cdot u)] \\
&\quad \times \left[M_{ll}^{(a)} M_{ll}^{(b)} \rho_l(k_1) \rho_l(k_2) + M_{tt}^{(a)} M_{tt}^{(b)} \rho_l(k_1) \rho_t(k_2) \right. \\
&\quad \left. + M_{ll}^{(a)} M_{ll}^{(b)} \rho_t(k_1) \rho_l(k_2) + M_{tt}^{(a)} M_{tt}^{(b)} \rho_t(k_1) \rho_t(k_2) \right],
\end{aligned} \tag{A.6}$$

where ρ_l and ρ_t are the spectral densities of the longitudinal and transverse components of the photon. The quantities $M^{(a,b)}$ are the contributions from the blobs; the subscripts denote appropriate components of the tensors. The analysis of [17] can be adapted to show that the term quadratic in ρ_t is the dominant infra-red term and gives the same contribution as that obtained with tree level propagators for the photon. Hence, hard thermal loop resummation does not change our results for Γ . Similar arguments hold for the production rate Γ_p . However, the leading terms, quadratic in ρ_t , cancel between the production and decay rates and hence the sub-leading terms become important for a reliable computation of the relaxation rate Γ_r . For this reason, hard thermal loop resummation becomes important for the computation of the radius and other properties of the axio-sphere.

References

- [1] R. D. Peccei and H. R. Quinn, *Phys. Rev. Lett.*, 38 (1977) 1440 and *Phys. Rev.*, D 16 (1977) 1791;
S. Weinberg, *Phys. Rev. Lett.*, 40 (1978) 223;
F. Wilczek, *Phys. Rev. Lett.*, 40 (1978) 279;
J. E. Kim, *Phys. Rev. Lett.*, 43 (1979) 103;
M. Zhitnitskii, *Sov. J. Nucl. Phys.*, 31 (1980) 260;
M. A. Shifman, A. I. Vainshtein, V. I. Zakharov, *Nucl. Phys.*, B 166 (1980) 493;
M. Dine, W. Fischler and M. Srednicki, *Phys. Lett.*, B 104 (1981) 199.
- [2] J. E. Kim, *Phys. Rep.*, 150 (1987) 1;
M. S. Turner, *Phys. Rep.*, 197 (1990) 67;
G. G. Raffelt, *Phys. Rep.*, 198 (1990) 1.
- [3] H. A. Weldon, *Phys. Rev.*, D 26 (1982) 1394.
- [4] E. Braaten and R. Pisarski, *Nucl. Phys.*, B 337 (1990) 569.
- [5] C. Contreras and M. Loewe, *Z. Phys.*, C 40 (1988) 253;
Bi Pin-Zhen and J. Rafelski, *Mod. Phys. Lett.*, A 7 (1992) 2493;
A. Gomez Nicola and R. F. Alvarez-Estrada, *Z. Phys.*, C 60 (1993) 711.
- [6] See for example, C. Itzykson and J. Zuber, *Quantum Field Theory*, McGraw Hill Book Company, New York, 1985.
- [7] N. P. Landsman and Ch. G. van Weert, *Phys. Rep.*, 145 (1987) 141.
- [8] L. Dolan and R. Jackiw, *Phys. Rev.*, D 9 (1974) 3312.
- [9] P. Sikivie, *Phys. Rev. Lett.*, 48 (1982) 1156;
M. S. Turner, *Phys. Rev.*, D 33 (1986) 889;
R. Davis, *Phys. Lett.*, B 180 (1986) 225;
D. Harari and P. Sikivie, *Phys. Lett.*, B 195 (1987) 361;
A. Dabholkar and J. M. Quashnock, *Nucl. Phys.*, B 333 (1990) 815.
- [10] A. S. Joshipura, *Int. J. Mod. Phys.*, A 7 (1992) 2021.
- [11] E. Kh. Akhmedov, Z. G. Berezhiani, R. N. Mohapatra and G. Senjanović, *Phys. Lett.*, B 299 (1993) 90.

- [12] J. Ellis and K. A. Olive, *Nucl. Phys.*, B 233 (1983) 252.
- [13] M. S. Turner, *Phys. Rev. Lett.*, 60 (1988) 1797;
R. Mayle *et al.*, *Phys. Lett.*, B 203 (1988) 188;
A. Burrows, M. S. Turner and R. P. Brinkmann, *Phys. Rev.*, D 39 (1989) 1020;
R. Mayle *et al.*, *Phys. Lett.*, B 219 (1989) 515.
- [14] P. Gerber and H. Leutwyler, *Nucl. Phys.*, B 321 (1989) 387.
- [15] R. L. Kobes and G. W. Semenoff, *Nucl. Phys.*, B 260 (1985) 714;
R. L. Kobes and G. W. Semenoff, *Nucl. Phys.*, B 272 (1986) 329;
F. Gelis, preprint hep-ph/9701410.
- [16] H. A. Weldon, *Phys. Rev.*, D 28 (1983) 2007.
- [17] R. Pisarski, *Physica*, A 158 (1989) 146.